Report

Cell Reports

Identification of Oxa1 Homologs Operating in the Eukaryotic Endoplasmic Reticulum

Graphical Abstract

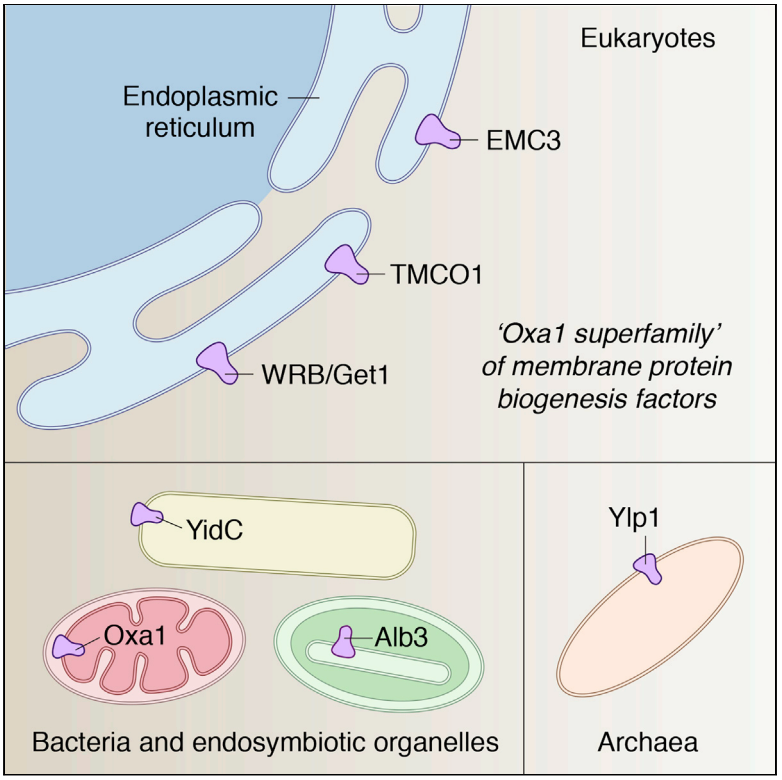

Highlights

- The "Oxa1 superfamily" comprises a group of membrane protein biogenesis factors
- Three ER-resident proteins, Get1, EMC3, and TMCO1, are members of the superfamily
- TMCO1, similar to bacterial YidC, associates with ribosomes and the Sec translocon

Authors

S. Andrei Anghel, Philip T. McGilvray, Ramanujan S. Hegde, Robert J. Keenan

Correspondence

bkeenan@uchicago.edu

In Brief

The absence of Oxa1/Alb3/YidC homologs in the eukaryotic endomembrane system has been a mystery. Now, Anghel et al. identify three ER-resident proteins, Get1, EMC3, and TMCO1, as remote homologs of Oxa1/Alb3/YidC proteins and show that TMCO1 possesses YidC-like biochemical properties. This defines the "Oxa1 superfamily" of membrane protein biogenesis factors.

Anghel et al., 2017, Cell Reports *21*, 3708–3716
December 26, 2017
https://doi.org/10.1016/j.celrep.2017.12.006

CellPress

OPEN ACCESS
CellPress

Cell Reports
Report

Identification of Oxa1 Homologs Operating in the Eukaryotic Endoplasmic Reticulum

S. Andrei Anghel,[1,2] Philip T. McGilvray,[1] Ramanujan S. Hegde,[3] and Robert J. Keenan[1,4,*]
[1]Department of Biochemistry and Molecular Biology
[2]Cell and Molecular Biology Graduate Program
The University of Chicago, 929 East 57th Street, Chicago, IL 60637, USA
[3]MRC Laboratory of Molecular Biology, Francis Crick Avenue, Cambridge CB2 0QH, UK
[4]Lead Contact
*Correspondence: bkeenan@uchicago.edu
https://doi.org/10.1016/j.celrep.2017.12.006

SUMMARY

Members of the evolutionarily conserved Oxa1/Alb3/YidC family mediate membrane protein biogenesis at the mitochondrial inner membrane, chloroplast thylakoid membrane, and bacterial plasma membrane, respectively. Despite their broad phylogenetic distribution, no Oxa1/Alb3/YidC homologs are known to operate in eukaryotic cells outside the endosymbiotic organelles. Here, we present bioinformatic evidence that the tail-anchored protein insertion factor WRB/Get1, the "endoplasmic reticulum (ER) membrane complex" subunit EMC3, and TMCO1 are ER-resident homologs of the Oxa1/Alb3/YidC family. Topology mapping and co-evolution-based modeling demonstrate that Get1, EMC3, and TMCO1 share a conserved Oxa1-like architecture. Biochemical analysis of human TMCO1, the only homolog not previously linked to membrane protein biogenesis, shows that it associates with the Sec translocon and ribosomes. These findings suggest a specific biochemical function for TMCO1 and define a superfamily of proteins—the "Oxa1 superfamily"—whose shared function is to facilitate membrane protein biogenesis.

INTRODUCTION

Membrane proteins must be inserted into the appropriate lipid bilayer to perform their biological functions and avoid toxic aggregation (Chiti and Dobson, 2006; Kopito, 2000). The existence of different types of membrane proteins and, in eukaryotes, different target membranes poses a challenge for the cellular biosynthetic machinery. To overcome this challenge, cells have evolved different pathways for insertion into membranes. The best understood of these is a co-translational pathway that delivers nascent polypeptides to the Sec translocon, a conserved proteinaceous channel in eukaryotes and prokaryotes. This pathway mediates insertion of most membrane proteins into the prokaryotic plasma membrane and the eukaryotic endoplasmic reticulum (ER) (Nyathi et al., 2013).

Some membrane proteins, however, are inserted independently of the translocon. For example, in eukaryotes, tail-anchored (TA) proteins are inserted into the ER membrane by the WRB-CAML complex (Get1-Get2 in yeast; Mariappan et al., 2011; Schuldiner et al., 2008; Vilardi et al., 2011; Wang et al., 2011, 2014; Yamamoto and Sakisaka, 2012). TA proteins are topologically simple, comprising a cytosolic-facing N-terminal domain and a single C-terminal transmembrane domain (TMD). The extreme C-terminal location of their TMD precludes targeting through the co-translational pathway. As a result, TA proteins utilize a Sec-independent post-translational pathway for insertion (Kutay et al., 1995; Stefanovic and Hegde, 2007). This pathway is conserved in eukaryotes, but whether it operates in bacteria and archaea remains unknown.

In bacteria, certain proteins are inserted into the plasma membrane by co- and post-translational, translocon-independent pathways mediated by YidC (Dalbey et al., 2014; Pross et al., 2016). These substrates are generally small, topologically simple proteins that lack large or highly charged translocated regions (Dalbey et al., 2014). YidC also functions in a translocon-dependent mode, where it facilitates the insertion, folding, and/or assembly of substrates containing multiple TMDs (Kuhn et al., 2017). Homologs of YidC are present in the mitochondrial inner membrane (called Oxa1 and Cox18) and the chloroplast thylakoid membrane (Alb3 and Alb4; Wang and Dalbey, 2011). Like bacterial YidC, these proteins function in different contexts as insertases, chaperones, and assembly factors.

Although YidC homologs are widely conserved among bacteria and archaea (Borowska et al., 2015), none have yet been identified in the eukaryotic endomembrane system. The absence of any such homolog has been puzzling, because the eukaryotic endomembrane system is derived from invagination of the plasma membrane of a prokaryotic ancestor (Cavalier-Smith, 2002). Here, we present evidence that the ER membrane possesses multiple proteins related to the Oxa1/Alb3/YidC family. These include the WRB/Get1 subunit of the TA protein insertase complex and two less understood but highly conserved proteins, TMCO1 and EMC3. We propose that these proteins are members of a superfamily—which we designate the "Oxa1 superfamily"—that all function broadly in membrane protein biogenesis.

RESULTS

Phylogenetic and Functional Comparisons Define the Oxa1 Superfamily

In searching for archaeal homologs of the TA membrane protein insertion factor WRB/Get1, we identified a family of archaeal and

A

HHpred

Query	Hits	Prob	#Aligned	% ID
WRB	Ylp1	99.0	163	12
	TMCO1	98.9	160	14
	EMC3	92.4	169	11
TMCO1	Ylp1	99.9	158	20
	WRB	99.8	156	19
	EMC3	99.5	184	15
	Oxa1	96.9	174	13
EMC3	TMCO1	99.9	188	16
	Ylp1	99.2	167	13
Ylp1	Oxa1	100	189	16
	Cox18	99.9	188	11
	TMCO1	99.9	157	20
	YidC	99.1	178	10
	EMC3	96.8	169	15
	WRB	95.0	155	12
Oxa1	Cox18	100	312	24
	YidC	100	288	22
	Ylp1	99.1	183	16

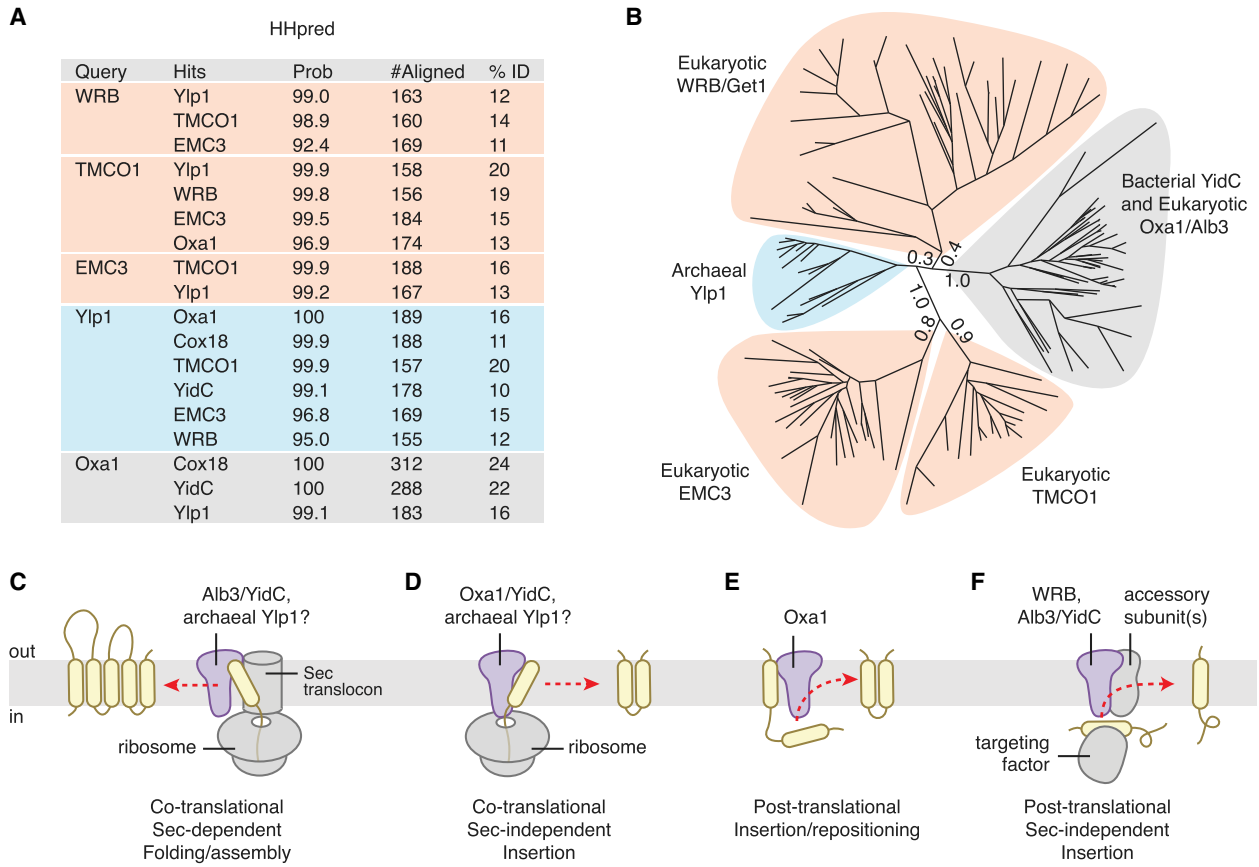

Figure 1. Phylogenetic and Functional Comparison Defines the Oxa1 Superfamily

(A) Identification of remote DUF106 homologs using HHpred. Eukaryotic (human), bacterial (*E. coli*), and archaeal (*M. jannaschii*) proteomes were searched for each query (UniProt ID: WRB, O00258; Oxa1, Q15070; TMCO1, Q9UM00; EMC3, Q9P0I2; Ylp1, Q57904) using default settings in HHpred in "global" alignment mode. Top hits are listed, along with the HHpred probability score, the number of residues aligned, and the sequence identity.

(B) Maximum-likelihood tree of representative sequences. Branch lengths for the five main clades are indicated.

(C) During Sec-dependent, co-translational assembly and folding, substrates are delivered to the membrane by the ribosome; insertion requires participation of the Sec translocon. Substrates of this pathway typically contain multiple TMDs and/or large translocated regions. Superfamily members exemplifying this activity include bacterial YidC and chloroplast Alb3.

(D) During Sec-independent, co-translational insertion, topologically "simple" substrates that lack large or highly charged translocated regions are delivered to the membrane by the ribosome. Superfamily members exemplifying this activity include Oxa1 and YidC; archaeal Ylp1 proteins function similarly *in vitro*.

(E) Post-translational TMD repositioning, exemplified by Oxa1.

(F) During Sec-independent, post-translational insertion, topologically simple substrates are delivered to the membrane by soluble targeting factors. Superfamily members exemplifying this activity include WRB/Get1, which inserts tail-anchored proteins delivered by TRC40/Get3; chloroplast Alb3, which inserts specific proteins delivered to the thylakoid membrane by cpSRP43; and bacterial YidC.

eukaryotic membrane proteins annotated as "domain of unknown function 106" (DUF106) that are distantly related to the Oxa1/Alb3/YidC family (Figures 1A and 1B). The DUF106 group includes an archaeal family of uncharacterized membrane proteins, the eukaryotic "ER membrane complex" (EMC) subunit 3 (EMC3) family, and the eukaryotic "transmembrane and coiled coil domains 1" (TMCO1) family. DUF106 proteins appear to be phylogenetically ancient, as they are present in the Asgard archaea, a group of organisms postulated to be the closest living relative of the last common ancestor of both archaeans and eukaryotes (Spang et al., 2015; Zaremba-Niedzwiedzka et al., 2017).

Consistent with these phylogenetic observations, there are clear functional similarities between members of the Oxa1/Alb3/YidC clade and members of the other clades for which some biochemical activity has been established (Figures 1C–1F). For example, during co-translational, translocon-independent insertion of a substrate protein into the bacterial plasma membrane, YidC binds to ribosome-nascent chain complexes (RNCs) and directly contacts the hydrophobic nascent chain (Kumazaki et al., 2014a, 2014b). Similarly, the archaeal DUF106 protein *Mj*0480 (henceforth called the "YidC-like protein 1" or Ylp1) binds RNCs and can be crosslinked to a model substrate *in vitro* (Borowska et al., 2015). Moreover, the known translocon-independent substrates of YidC and Oxa1 and the post-translational substrates of Alb3 and WRB/Get1 are all simple membrane proteins with few transmembrane helices and small translocated regions (Aschtgen et al., 2012; Hegde and

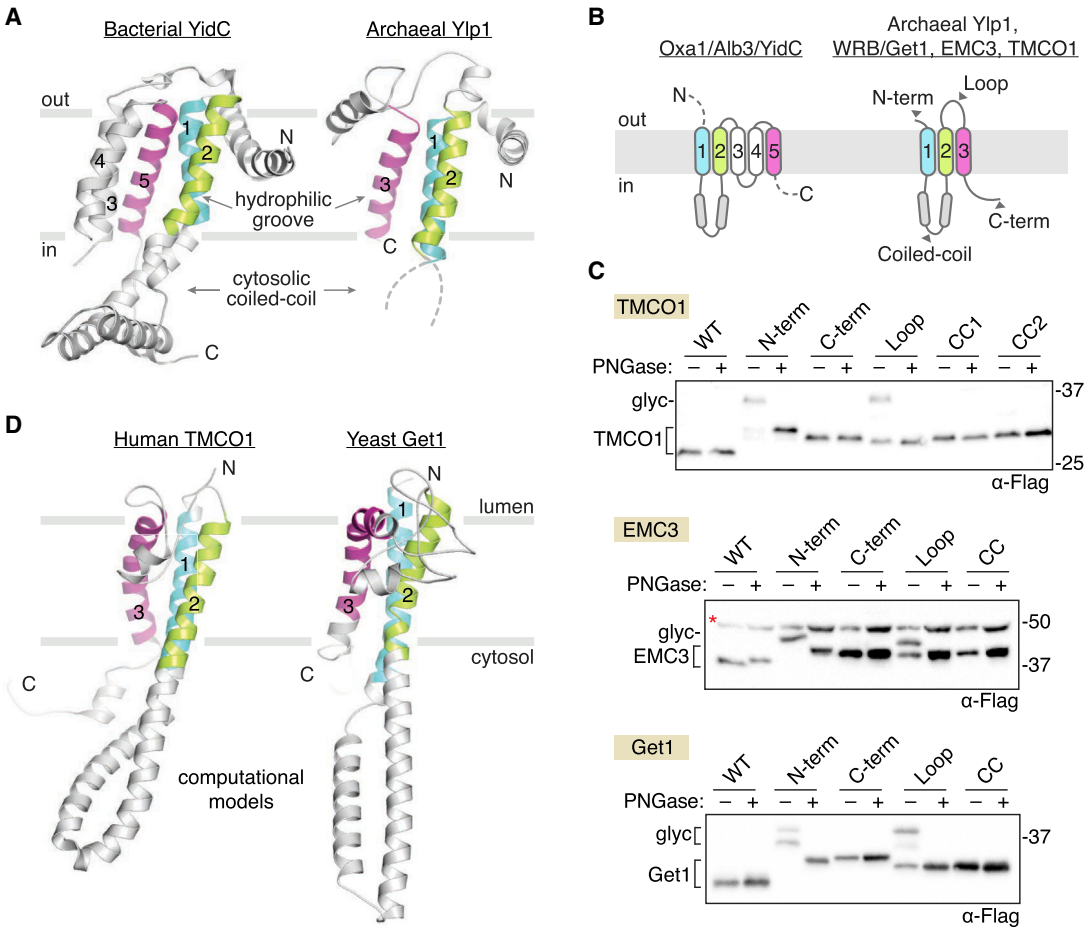

Figure 2. Oxa1 Superfamily Members Share a Conserved Membrane Topology and Core Structural Features

(A) Comparison of known structures from two clades: bacterial YidC (left; PDB 3WO6) and archaeal Ylp1 (right; PDB 5C8J). These proteins share a common N-out/C-in topology, a cytosolic-facing coiled coil between TM1 and TM2 (disordered in the archaeal structure), and a three-TMD core (colored) that harbors a lipid-exposed hydrophilic groove implicated in binding to nascent polypeptides during insertion.

(B) Predicted topology of the Oxa1 superfamily members.

(C) Experimentally defined topology of human TMCO1, EMC3, and yeast Get1. Glycosylation acceptor sequences were introduced at the indicated positions (gray arrowheads in B and Figure S2), and glycosylation was monitored by western blotting after treatment with or without PNGase F. All three proteins conform to the predicted Oxa1 superfamily topology. A non-specific, cross-reacting band visible in all EMC3 samples is marked (red asterisk).

(D) Evolutionary covariation-based computational 3D models of human TMCO1 and yeast Get1 recapitulate the core structural features of bacterial YidC and archaeal Ylp1: lumenal N terminus; cytosolic-facing coiled coil and C terminus; and a three-TMD core. Here, the predicted coiled coil region of Get1 has been replaced with the experimentally determined structure of the Get1 coiled coil (PDB 3ZS8). The resulting hybrid model is in good agreement with the covariation-based 3D model calculated for human WRB (Figure S2).

See also Figures S1 and S2.

Keenan, 2011; Wang and Dalbey, 2011). Finally, although its precise function remains to be defined, the EMC has been linked to ERAD and biosynthesis of multi-pass membrane proteins (Richard et al., 2013; Satoh et al., 2015). Given these phylogenetic and functional similarities, we propose to assign these proteins as members of a superfamily, which we hereafter refer to as the Oxa1 superfamily.

Oxa1 Superfamily Members Share Topological and Structural Features

A key prediction is that, owing to their common ancestry and conserved function, all members of the Oxa1 superfamily share a common architecture. As noted previously (Borowska et al., 2015), comparison of the crystal structures of bacterial YidC (Kumazaki et al., 2014a, 2014b) and archaeal Ylp1 (Borowska et al., 2015) reveals considerable structural overlap, including a three-TMD core, an N-in/C-out orientation, a cytosolic coiled coil between the first two TMDs, and a lipid-exposed hydrophilic groove, which has been shown to contact substrate proteins (Figure 2A).

Secondary structure and topology predictions for Get1, TMCO1, and EMC3 suggest they share this architecture (Figures 2B and S1), but the topology of these proteins has not been conclusively established. Indeed, a recent study proposed that

TMCO1 has an N-in/C-in topology, with only two TMDs and a lumenal-facing coiled coil (Wang et al., 2016); this topology is incompatible with placement of TMCO1 into the Oxa1 superfamily.

To define the topology of Get1, TMCO1, and EMC3, we designed 3×Flag-tagged constructs containing a consensus glycosylation sequence at the N or C terminus or within the predicted cytosolic coiled coil or lumenal loop regions (Figures 2B and S2A). In all cases, we observed glycosylation of the N terminus and the loop between the second and third TMDs and no glycosylation of the C terminus or the coiled coil domain (Figure 2C). These data are consistent with the observation that the Get1 coiled coil binds to the cytosolic targeting machinery (Mariappan et al., 2011; Stefer et al., 2011; Wang et al., 2011) and with proteomic analyses showing that serine residues in the coiled coil and C-terminal regions of TMCO1 are phosphorylated by cytosolic kinases (Dephoure et al., 2008; Olsen et al., 2010).

We also performed an unbiased, 3D structure prediction of TMCO1, Get1, and EMC3 using distance restraints derived from evolutionarily coupled residue pairs (Wang et al., 2017). Remarkably, the top-ranked models for human TMCO1 and yeast Get1 recapitulated the core structural features of bacterial YidC and archaeal Ylp1 proteins, including a lumenal N terminus, cytosolic-facing coiled coil and C terminus, and a three-TMD core (Figures 2D, S2B, and S2D). The top-ranked EMC3 models also possessed a three-TMD core and a coiled coil motif between the first two TMDs but showed physically implausible orientations for the coiled coil and C terminus (Figure S2C); this may reflect the limited number of available sequence homologs, the relatively larger size of EMC3, and the absence of any membrane bilayer energy term. Nevertheless, these models suggest that members of the Oxa1 superfamily share a membrane topology and core architecture.

TMCO1 Interacts with the Ribosome and the Sec61 Translocon

A second prediction of the Oxa1 superfamily model is that all of the proteins function in some capacity in membrane protein biogenesis. To test this prediction, we focused on human TMCO1, the only member of the superfamily not yet linked to membrane protein biogenesis. TMCO1 is an ER-resident membrane protein that is conserved in most eukaryotes (Iwamuro et al., 1999). Genetic variations around *TMCO1* are linked to glaucoma (Burdon et al., 2011; Sharma et al., 2012), and nonsense mutations cause a disorder associated with craniofacial dysmorphisms, skeletal anomalies, and intellectual disability (Alanay et al., 2014; Caglayan et al., 2013; Xin et al., 2010).

We asked whether any of the interactions of TMCO1 are similar to those of the better characterized members of the Oxa1 superfamily. In the case of bacterial YidC, primary interaction partners include the Sec translocon and the ribosome (Figures 1C and 1D). We first explored whether TMCO1 is part of a complex with translating ribosomes, as would be expected if it functions in co-translational insertion like some members of the Oxa1 superfamily (Figures 1C and 1D).

When digitonin-solubilized HEK293 membranes were fractionated on a sucrose gradient, TMCO1 and Sec61 were present in the 80S ribosome fraction (Figure 3A). In contrast, Derlin-1, an abundant ER membrane protein not known to bind the ribosome, did not co-migrate with ribosomes. Next, we tested whether TMCO1 and Sec61 are part of the same ribosome-bound complex. After immunoprecipitating digitonin-solubilized membranes prepared from a 3×Flag-tagged TMCO1 HEK293 cell line (Figure S3A), we observed a complex containing TMCO1, Sec61, and ribosomes (Figure 3B). Thus, TMCO1-Sec61-ribosome complexes can be isolated from cells under native conditions.

We next explored whether TMCO1 can exist in complex with Sec61 in the absence of ribosomes, as is true for YidC (Botte et al., 2016; Duong and Wickner, 1997). To identify ribosome-independent complexes, we used antibodies that bind TMCO1 and Sec61β on epitopes expected to be occluded by a bound ribosome. After immunoprecipitating digitonin-solubilized canine pancreatic microsomes (which contain high levels of Sec61), the anti-TMCO1 antibody pulled down components of the Sec61 translocon (Figure 3C). As expected, none of the antibodies pulled down ribosomes or the control protein, Derlin-1. This suggests that TMCO1 and Sec61 can exist in the same complex in the absence of ribosomes.

Finally, we asked whether TMCO1 has an intrinsic affinity for ribosomes, as is the case for Oxa1 and some YidC homologs with long, positively charged C-terminal regions (Jia et al., 2003; Seitl et al., 2014). To test this prediction, we incubated recombinant, purified TMCO1 (Figure S3B) with unprogrammed ribosomes isolated from rabbit reticulocyte lysate. After sedimentation through a sucrose cushion, we observed ribosome-dependent pelleting of TMCO1 (Figure 3D). This interaction was salt sensitive, could be stabilized by chemical crosslinking, and was specific, because high concentrations of bulk RNA did not disrupt the interaction (Figures 3D, S3C, and S3D). Thus, in addition to its conserved structural features, TMCO1 shares key functional properties with members of the Oxa1/Alb3/YidC family, consistent with the predictions of the Oxa1 superfamily hypothesis.

DISCUSSION

Our phylogenetic, topological, and functional data identify an unexpected evolutionary relationship among a diverse group of integral membrane proteins that together define the Oxa1 superfamily. These proteins include bacterial YidC and its homologs in mitochondria and chloroplasts, archaeal Ylp1 proteins, and three ER-resident proteins: WRB/Get1; EMC3; and TMCO1. The best characterized members of the superfamily function in membrane protein biogenesis (Figures 1C–1F). In particular, Oxa1/Alb3/YidC proteins facilitate the insertion, folding, and/or assembly of a variety of membrane proteins (Wang and Dalbey, 2011), whereas the WRB/Get1 subunit of the GET pathway transmembrane complex mediates the insertion of TA membrane proteins into the ER (Hegde and Keenan, 2011). Similarly, the EMC3 subunit of the ER membrane complex has been proposed to play a role in membrane protein quality control (Richard et al., 2013) and biogenesis (Satoh et al., 2015).

The function of TMCO1 has been less clear. Here, we show that TMCO1 possesses an Oxa1-like architecture and that TMCO1-Sec61-ribosome complexes can be isolated from

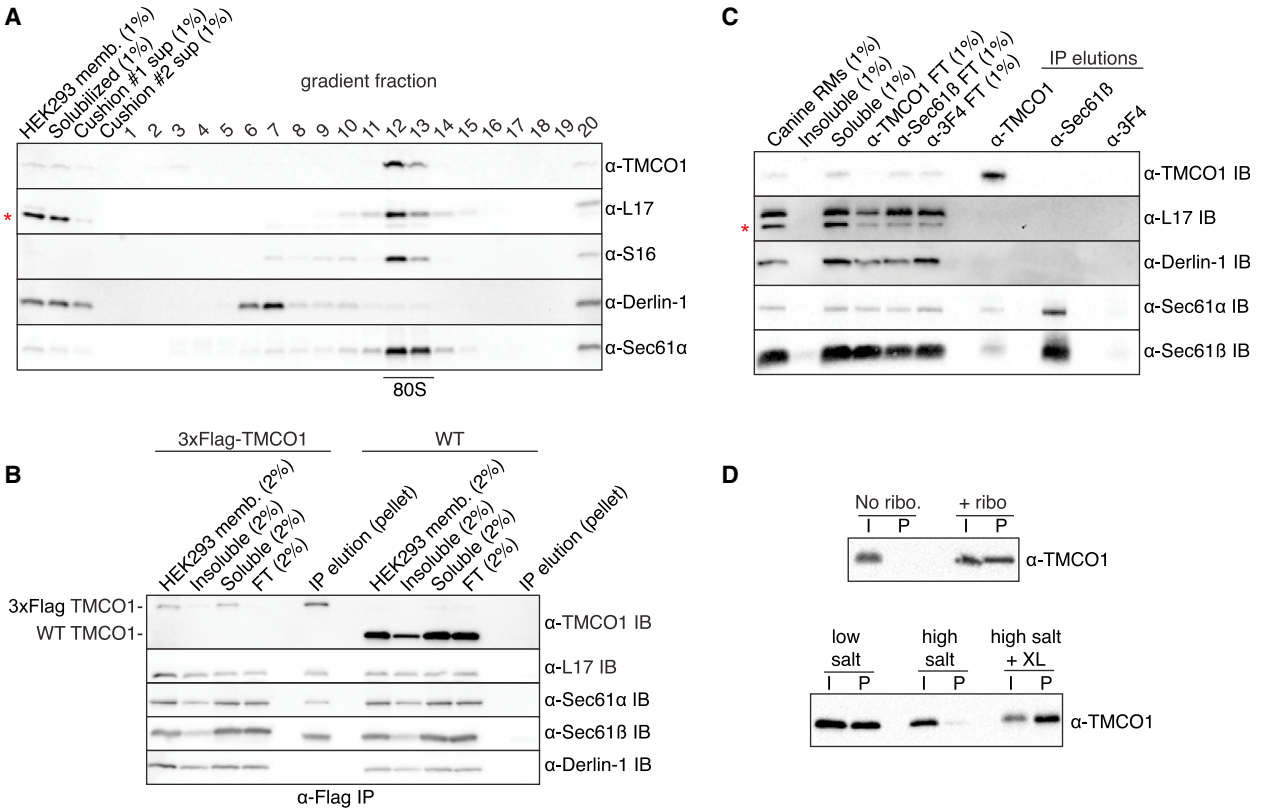

Figure 3. TMCO1 Forms a Complex with the Sec61 Translocon and RNCs

(A) HEK293 membranes were solubilized with digitonin, fractionated by sucrose cushion, separated on a high-resolution sucrose gradient, and analyzed by western blotting. TMCO1 co-fractionates with intact 80S particles and the Sec61 translocon, but not the unrelated ER membrane protein Derlin-1, which does not bind to ribosomes. Blots for the large (L17) and small (S16) ribosomal subunits are also shown; a non-specific, cross-reacting band visible in the L17 blot is indicated with an asterisk.

(B) Digitonin-solubilized membranes from wild-type (WT) HEK293 cells or a HEK293 cell line containing an N-terminal 3×Flag-tagged TMCO1 allele were analyzed by anti-Flag immunoprecipitation, sucrose cushion, and western blotting.

(C) Digitonin-solubilized canine pancreatic rough microsomes were tested for interaction between TMCO1 and Sec61 by co-immunoprecipitation and western blotting. An anti-TMCO1, but not a control anti-3F4 antibody, pulls down two components of Sec61. The absence of TMCO1 in the reciprocal pull-down is consistent with the higher levels of Sec61 in these membranes.

(D) Recombinant, purified TMCO1 co-sediments with unprogrammed ribosomes isolated from rabbit reticulocyte lysate (top panel). This interaction is salt sensitive and can be stabilized by chemical crosslinking (XL) (bottom panel). The pellet (P) fractions correspond to 5× volume equivalents of the input (I) fractions. See also Figure S3.

HEK293 cells under native conditions. We also show that TMCO1 can be isolated in ribosome-free complexes with Sec61 and that TMCO1 has an intrinsic affinity for ribosomes. These properties suggest that TMCO1 functions most analogously to bacterial YidC and may facilitate the co-translational insertion, folding, and/or assembly of newly synthesized membrane proteins into the ER membrane (Figures 1C and 1D).

This assignment is not incompatible with the previous proposal that TMCO1 functions as a Ca^{2+} channel (Wang et al., 2016). Indeed, other well-characterized membrane protein insertases, including the bacterial and eukaryotic Sec translocon (Sachelaru et al., 2017; Simon and Blobel, 1991; Simon et al., 1989; Wirth et al., 2003) and mitochondrial Oxa1 (Krüger et al., 2012), have also been shown to conduct ions. This activity is likely related to their ability to translocate polypeptides across a membrane bilayer, and the same may be true for TMCO1. Alternatively, TMCO1 may modulate the Ca^{2+} efflux properties of Sec61 (Erdmann et al., 2011; Lang et al., 2011) or facilitate the biogenesis of a protein that functions in Ca^{2+} transport.

We speculate that Oxa1 superfamily proteins are all descendants of an ancestral machine that could insert topologically "simple" membrane proteins into the bilayer. Over time, the need to handle more complex substrates with additional TMDs and/or larger translocated regions would have been satisfied by evolution of the translocon. Subsequently, Oxa1 superfamily members would have been freed to evolve more specialized functions in concert with other membrane-bound and soluble factors. This might manifest in the translocon-dependent chaperone activities of YidC and Alb3 and the evolution of eukaryotic WRB/Get1 and EMC3 to function in association with other integral membrane components. Likewise, adaptation of WRB/Get1 and Alb3 to post-translational insertion would have resulted from

modification of their cytosolic-facing coiled coil and C terminus for binding to the TRC40/Get3- and cpSRP54-targeting factors, respectively, instead of the ribosome.

The Oxa1 superfamily illustrates how a single structural scaffold has been diversified to handle the insertion, folding, and assembly of different proteins into different cellular membranes. The shared characteristics of Oxa1/Alb3/YidC and WRB/Get1 translocon-independent substrates raises the possibility that Oxa1 superfamily members might, under certain circumstances, act on overlapping sets of substrates in the ER. Consistent with this idea, it is notable that disruption of WRB (Sojka et al., 2014; Vogl et al., 2016), TMCO1 (Caglayan et al., 2013; Xin et al., 2010), or EMC3 (Ma et al., 2015) is non-lethal. Such functional redundancy would impart robustness to membrane protein biogenesis, particularly under conditions of stress (Aviram et al., 2016; Aviram and Schuldiner, 2014). Identifying the native substrates and molecular mechanisms underlying EMC3- and TMCO1-mediated biogenesis are important topics for future investigation.

EXPERIMENTAL PROCEDURES

Phylogenetic Analysis

The DUF106 protein from *M. jannaschii* (*MJ*0480/Ylp1) was identified by HHpred (Söding et al., 2005) as a remote archaeal homolog of eukaryotic WRB/Get1. Expanded searches of eukaryotic, bacterial, and archaeal proteomes subsequently revealed a set of remote homologs, including Oxa1/Alb3/YidC, WRB/Get1, EMC3, TMCO1, and archaeal Ylp1 proteins (Figure 1).

For each of these protein families, homologs were retrieved using PSI-Blast (Altschul et al., 1997) with an expected threshold cutoff of 10^{-1}. An effort was made to include organisms as phylogenetically diverse as possible. Proteins in this list were then aligned using MUSCLE (Edgar, 2004). Gaps in the alignment were trimmed using TrimAl (Capella-Gutiérrez et al., 2009) with a cutoff of 0.4. A maximum-likelihood phylogenetic tree was built using PhyML-SMS (Guindon and Gascuel, 2003) using nearest-neighbor interchange (NNI) and the Akaike information criterion.

TMCO1 and EMC3 Topology Analysis by Glycosylation Mapping

An N-terminally 3×Flag-tagged human TMCO1 construct, codon-optimized for bacterial expression, was subcloned into the pGFP plasmid (Clontech). EMC3 plasmids were identical but contained a cDNA-derived EMC3 sequence. The resulting constructs encode a 3×Flag-tagged protein under the control of a cytomegalovirus (CMV) promoter and an SV40 polyA signal. An opsin N-glycosylation tag (MNGTEGPNFYVPFSNKTVD) was then inserted at the indicated positions (Figure S2A). Transfections were performed by mixing 10 μg of DNA with 20 μL of Trans-It 293 reagent (Mirus Bio) in serum-free DMEM medium, incubating for 20 min at room temperature, and then adding to one 10-cm cell culture dish of HEK293 TRex TMCO1 KO (for TMCO1 transfections) or HEK293 TRex cells (for EMC3 transfection) at ~90% confluency. Cells were subcultivated 1:2 the next day and harvested 48 hr after transfection.

The membrane fraction was prepared as described in the Supplemental Experimental Procedures. The membranes were resuspended in 100 μL of 1% SDS with 100 mM DTT, incubated for 5 min at 95°C, and then cooled at room temperature. Buffer was adjusted to 50 mM HEPES (pH 7.4), 150 mM NaCl, 1% NP40, and 0.1% SDS and supplemented with 50 units of Benzonase (Sigma; E1014) and then split in half and treated with or without 20 units of PNGase F (Promega). Reactions were incubated for 4 hr at 37°C and then trichloroacetic acid (TCA) precipitated, resuspended in Laemmli Sample Buffer, and analyzed by SDS-PAGE.

Get1 Topology Analysis by Glycosylation Mapping

A C-terminally 3×Flag-tagged *S. cerevisiae* Get1 sequence was subcloned into Yeplac195 under the control of the endogenous promoter and a CYC1 terminator. The opsin N-glycosylation tag was inserted at the indicated positions (Figure S2A). Plasmids were transformed into BY4741 yeast using the lithium acetate method (Gietz and Woods, 2002).

For glycosylation mapping experiments, yeast cells were picked off selective plates and grown for 1 hr in SD −URA +2% glucose at room temperature with 225 rpm shaking. Four A_{600} units were then collected and mixed with sodium azide to a final concentration of 0.01%, placed on ice, and lysed through a modified alkaline lysis method (Kushnirov, 2000). Cells were collected by centrifuging 3 min at 16,000 × *g* and then resuspended in 350 mM freshly diluted NaOH supplemented with 1 mM PMSF and 1× cOmplete, Mini, EDTA-free Protease Inhibitor Cocktail tablets (Roche). After a 5-min incubation on ice, cells were collected by centrifuging 3 min at 16,000 × *g* and the supernatant was discarded. The cell pellet was resuspended in 120 μL of 1% SDS, 100 mM DTT, and 50 mM Tris (pH 6.8) and incubated for 5 min at 95°C, cooled to room temperature, and centrifuged 3 min at 16,000 × *g* to remove insoluble material. Only the supernatant was processed further. Buffer was adjusted to 5 mM Tris (pH 6.8), 50 mM HEPES (pH 7.4), 150 mM NaCl, 1% NP40, and 0.1% SDS and supplemented with 25 units of Benzonase (Sigma; E1014), split in half, and then treated with or without 20 units of PNGase F (Promega). Reactions were incubated for 4 hr at 37°C and then TCA precipitated, resuspended in Laemmli Sample Buffer, and analyzed by SDS-PAGE.

TMD Prediction and 3D Modeling

Transmembrane domain predictions were made with PolyPhobius (Käll et al., 2005) and TOPCONS (Tsirigos et al., 2015); coiled coil predictions were made with COILS (Lupas et al., 1991). RaptorX-Contact (Wang et al., 2017) was used to calculate contact maps from alignments of 584 TMCO1 (188 residues), 453 EMC3 (261 residues), 442 Get1 (235 residues), and 485 WRB (174 residues) sequences from different species. RaptorX-Contact uses sequence conservation, residue co-evolution, and contact occurrence patterns to improve contact prediction in difficult cases like these, where only relative few sequence homologs are available. Template-free 3D modeling was done in CNS (Brünger et al., 1998) using the predicted contacts as distance restraints, as implemented in the http://raptorx.uchicago.edu/ContactMap/ web server.

The 3D models for yeast Get1 and EMC3 show distortions in the highly charged coiled coil (Get1 and EMC3) and C-terminal regions (EMC3). In particular, these regions are observed to bend backward into the bilayer rather than extending away from it (Figures S2B and S2C). These non-physiologic conformations likely reflect the inclusion of a spurious restraint(s) in the 3D modeling, which does not explicitly account for the membrane (Wang et al., 2017). Thus, we constructed a hybrid model of Get1, in which the distorted coiled coil was replaced with the crystallographically defined Get1 coiled coil (PDB 3ZS8) by manually docking it as a rigid body between TM1 and TM2 (Figure 2D). Notably, in a covariation-based 3D model of WRB (the human homolog of Get1), the coiled coil adopts an energetically reasonable conformation (Figure S2B). No attempt was made to model EMC3 further, because no structural information is available for this protein.

Assay for *In Vivo* Association of TMCO1 with Ribosomes

The total HEK293 cell membrane fraction (in assay buffer: 150 mM potassium acetate; 50 mM HEPES [pH 7.4]; and 5 mM magnesium acetate) was solubilized by addition of recrystallized digitonin (Calbiochem; lot no. 2913883) from a 5% stock to a final concentration of 2%. Solubilization was allowed to proceed for 30 min at 4°C with end over end mixing and then insoluble material was removed by centrifugation for 10 min at 10,000 × *g*. The soluble material was then layered over a 1-mL sucrose cushion (150 mM KCl, 50 mM Tris [pH 7.4], 5 mM MgCl2, 1 M sucrose, and 0.1% digitonin). Sucrose cushions were pelleted for 2 hr at 250,000 × *g* in a TLA100.3 rotor (Belin et al., 2010). The pellet was resuspended in the same buffer, re-run over a cushion again, and then finally the resuspended pellet was pelleted through a gradient (10%–50% sucrose, 150 mM potassium acetate, 50 mM Tris [pH 7.5], 5 mM MgCl2, and 0.1% digitonin) at 130,000 × *g* (SW28.1; Beckman Coulter) for 12 hr at 4°C. 900 μL fractions were collected manually from the top of the gradient, TCA precipitated, and analyzed by SDS-PAGE.

Co-immunoprecipitation Analyses

For co-immunoprecipitations from canine pancreatic membranes (Promega), the membranes were resuspended in a buffer containing 250 mM potassium

acetate, 50 mM HEPES (pH 7.4), 5 mM magnesium acetate, 15% glycerol, and 3% recrystallized digitonin (Calbiochem; Kun et al., 1979). Solubilization was allowed to proceed for 30 min on ice, and then insoluble material was removed by centrifugation for 10 min at 10,000 × *g*. The soluble material was then divided equally and layered over protein A resin that had been crosslinked to antibodies against TMCO1, Sec61β, or 3F4 (as control). Immunoprecipitation (IP) reactions were incubated for 2 hr at 4°C with end-over-end mixing and then washed six times with 250 mM potassium acetate, 50 mM HEPES (pH 7.4), 5 mM magnesium acetate, 15% glycerol, and 0.1% digitonin. Bound proteins were eluted by three successive 10-min incubations with 1 M glycine (pH 3) supplemented with 0.1% Fos-choline-12. Elutions were then TCA precipitated, resuspended in Laemmli Sample Buffer, and analyzed by SDS-PAGE.

For co-immunoprecipitations from 3×Flag-TMCO1 HEK293 TRex cells, the membrane fraction was isolated and washed twice with 250 mM potassium acetate, 50 mM HEPES (pH 7.4), 10 mM magnesium acetate, and 250 mM sucrose. Membranes were then resuspended in buffer containing 250 mM sucrose, 300 mM potassium acetate, 50 mM HEPES (pH 7.4), and 10 mM magnesium acetate. Solubilization was allowed to proceed for 30 min on ice, and then insoluble material was removed by centrifugation for 10 min at 10,000 × *g*. The soluble fraction was then added to anti-Flag M2 resin (Sigma) and incubated for 1 hr at 4°C with end-over-end mixing and then washed four times with 350 mM potassium acetate, 50 mM HEPES (pH 7.4), 5 mM magnesium acetate, 250 mM sucrose, and 0.1% digitonin. Bound proteins were eluted by 2 successive 30-min incubations with same buffer as the wash but supplemented with 0.5 mg/mL 3×Flag peptide (ApexBio). The elutions were then layered over a 1-mL sucrose cushion (150 mM KCl, 50 mM Tris [pH 7.4], 5 mM $MgCl_2$, 1 M sucrose, and 0.1% digitonin) and then pelleted for 2 hr at 250,000 × *g* at 4°C in a TLA100.3 rotor (Belin et al., 2010). The supernatant was discarded, and the ribosome pellet was resuspended in 2× Laemmli Sample Buffer for analysis.

SUPPLEMENTAL INFORMATION

Supplemental Information includes Supplemental Experimental Procedures and three figures and can be found with this article online at https://doi.org/10.1016/j.celrep.2017.12.006.

ACKNOWLEDGMENTS

We thank T. Starr for advice with the phylogenetic tree construction; B. Zalisko for digitonin recrystallization; R. Rock, D.A. Drummond, and F. Bezanilla for sharing equipment; D. Bishop for the yeast strain; and Keenan and Hegde lab members for advice. This work was supported by NIH R21 EY026719 (to R.J.K.) and the UK Medical Research Council MC_UP_A022_1007 (to R.S.H.). S.A.A. was supported by a Boehringer Ingelheim Fonds Ph.D. fellowship, and P.T.M. was supported by NIH training grant T32 GM007183.

AUTHOR CONTRIBUTIONS

R.S.H. and R.J.K. conceived of the project. S.A.A. and P.T.M. performed experiments. S.A.A. and R.J.K. wrote the manuscript with input from all authors.

DECLARATION OF INTERESTS

The authors declare no competing interests.

Received: May 17, 2017
Revised: October 18, 2017
Accepted: December 1, 2017
Published: December 26, 2017

REFERENCES

Alanay, Y., Ergüner, B., Utine, E., Haçarız, O., Kiper, P.O.S., Taşkıran, E.Z., Perçin, F., Uz, E., Sağıroğlu, M.Ş., Yuksel, B., et al. (2014). TMCO1 deficiency causes autosomal recessive cerebrofaciothoracic dysplasia. Am. J. Med. Genet. A. *164*, 291–304.

Altschul, S.F., Madden, T.L., Schäffer, A.A., Zhang, J., Zhang, Z., Miller, W., and Lipman, D.J. (1997). Gapped BLAST and PSI-BLAST: a new generation of protein database search programs. Nucleic Acids Res. *25*, 3389–3402.

Aschtgen, M.S., Zoued, A., Lloubès, R., Journet, L., and Cascales, E. (2012). The C-tail anchored TssL subunit, an essential protein of the enteroaggregative Escherichia coli Sci-1 Type VI secretion system, is inserted by YidC. MicrobiologyOpen *1*, 71–82.

Aviram, N., and Schuldiner, M. (2014). Embracing the void–how much do we really know about targeting and translocation to the endoplasmic reticulum? Curr. Opin. Cell Biol. *29*, 8–17.

Aviram, N., Ast, T., Costa, E.A., Arakel, E.C., Chuartzman, S.G., Jan, C.H., Haßdenteufel, S., Dudek, J., Jung, M., Schorr, S., et al. (2016). The SND proteins constitute an alternative targeting route to the endoplasmic reticulum. Nature *540*, 134–138.

Belin, S., Hacot, S., Daudignon, L., Therizols, G., Pourpe, S., Mertani, H.C., Rosa-Calatrava, M., and Diaz, J.J. (2010). Purification of ribosomes from human cell lines. Curr. Protoc. Cell Biol. *Chapter 3*, Unit 3.40.

Borowska, M.T., Dominik, P.K., Anghel, S.A., Kossiakoff, A.A., and Keenan, R.J. (2015). A YidC-like protein in the archaeal plasma membrane. Structure *23*, 1715–1724.

Botte, M., Zaccai, N.R., Nijeholt, J.L., Martin, R., Knoops, K., Papai, G., Zou, J., Deniaud, A., Karuppasamy, M., Jiang, Q., et al. (2016). A central cavity within the holo-translocon suggests a mechanism for membrane protein insertion. Sci. Rep. *6*, 38399.

Brünger, A.T., Adams, P.D., Clore, G.M., DeLano, W.L., Gros, P., Grosse-Kunstleve, R.W., Jiang, J.S., Kuszewski, J., Nilges, M., Pannu, N.S., et al. (1998). Crystallography & NMR system: a new software suite for macromolecular structure determination. Acta Crystallogr. D Biol. Crystallogr. *54*, 905–921.

Burdon, K.P., Macgregor, S., Hewitt, A.W., Sharma, S., Chidlow, G., Mills, R.A., Danoy, P., Casson, R., Viswanathan, A.C., Liu, J.Z., et al. (2011). Genome-wide association study identifies susceptibility loci for open angle glaucoma at TMCO1 and CDKN2B-AS1. Nat. Genet. *43*, 574–578.

Caglayan, A.O., Per, H., Akgumus, G., Gumus, H., Baranoski, J., Canpolat, M., Calik, M., Yikilmaz, A., Bilguvar, K., Kumandas, S., and Gunel, M. (2013). Whole-exome sequencing identified a patient with TMCO1 defect syndrome and expands the phenotic spectrum. Clin. Genet. *84*, 394–395.

Capella-Gutiérrez, S., Silla-Martínez, J.M., and Gabaldón, T. (2009). trimAl: a tool for automated alignment trimming in large-scale phylogenetic analyses. Bioinformatics *25*, 1972–1973.

Cavalier-Smith, T. (2002). The phagotrophic origin of eukaryotes and phylogenetic classification of Protozoa. Int. J. Syst. Evol. Microbiol. *52*, 297–354.

Chiti, F., and Dobson, C.M. (2006). Protein misfolding, functional amyloid, and human disease. Annu. Rev. Biochem. *75*, 333–366.

Dalbey, R.E., Kuhn, A., Zhu, L., and Kiefer, D. (2014). The membrane insertase YidC. Biochim. Biophys. Acta *1843*, 1489–1496.

Dephoure, N., Zhou, C., Villén, J., Beausoleil, S.A., Bakalarski, C.E., Elledge, S.J., and Gygi, S.P. (2008). A quantitative atlas of mitotic phosphorylation. Proc. Natl. Acad. Sci. USA *105*, 10762–10767.

Duong, F., and Wickner, W. (1997). Distinct catalytic roles of the SecYE, SecG and SecDFyajC subunits of preprotein translocase holoenzyme. EMBO J. *16*, 2756–2768.

Edgar, R.C. (2004). MUSCLE: multiple sequence alignment with high accuracy and high throughput. Nucleic Acids Res. *32*, 1792–1797.

Erdmann, F., Schäuble, N., Lang, S., Jung, M., Honigmann, A., Ahmad, M., Dudek, J., Benedix, J., Harsman, A., Kopp, A., et al. (2011). Interaction of calmodulin with Sec61α limits Ca2+ leakage from the endoplasmic reticulum. EMBO J. *30*, 17–31.

Gietz, R.D., and Woods, R.A. (2002). Transformation of yeast by lithium acetate/single-stranded carrier DNA/polyethylene glycol method. Methods Enzymol. *350*, 87–96.

Guindon, S., and Gascuel, O. (2003). A simple, fast, and accurate algorithm to estimate large phylogenies by maximum likelihood. Syst. Biol. *52*, 696–704.

Hegde, R.S., and Keenan, R.J. (2011). Tail-anchored membrane protein insertion into the endoplasmic reticulum. Nat. Rev. Mol. Cell Biol. *12*, 787–798.

Iwamuro, S., Saeki, M., and Kato, S. (1999). Multi-ubiquitination of a nascent membrane protein produced in a rabbit reticulocyte lysate. J. Biochem. *126*, 48–53.

Jia, L., Dienhart, M., Schramp, M., McCauley, M., Hell, K., and Stuart, R.A. (2003). Yeast Oxa1 interacts with mitochondrial ribosomes: the importance of the C-terminal region of Oxa1. EMBO J. *22*, 6438–6447.

Käll, L., Krogh, A., and Sonnhammer, E.L. (2005). An HMM posterior decoder for sequence feature prediction that includes homology information. Bioinformatics *21* (*Suppl 1*), i251–i257.

Kopito, R.R. (2000). Aggresomes, inclusion bodies and protein aggregation. Trends Cell Biol. *10*, 524–530.

Krüger, V., Deckers, M., Hildenbeutel, M., van der Laan, M., Hellmers, M., Dreker, C., Preuss, M., Herrmann, J.M., Rehling, P., Wagner, R., and Meinecke, M. (2012). The mitochondrial oxidase assembly protein1 (Oxa1) insertase forms a membrane pore in lipid bilayers. J. Biol. Chem. *287*, 33314–33326.

Kuhn, A., Koch, H.G., and Dalbey, R.E. (2017). Targeting and insertion of membrane proteins. Ecosal Plus *7*.

Kumazaki, K., Chiba, S., Takemoto, M., Furukawa, A., Nishiyama, K., Sugano, Y., Mori, T., Dohmae, N., Hirata, K., Nakada-Nakura, Y., et al. (2014a). Structural basis of Sec-independent membrane protein insertion by YidC. Nature *509*, 516–520.

Kumazaki, K., Kishimoto, T., Furukawa, A., Mori, H., Tanaka, Y., Dohmae, N., Ishitani, R., Tsukazaki, T., and Nureki, O. (2014b). Crystal structure of Escherichia coli YidC, a membrane protein chaperone and insertase. Sci. Rep. *4*, 7299.

Kun, E., Kirsten, E., and Piper, W.N. (1979). Stabilization of mitochondrial functions with digitonin. Methods Enzymol. *55*, 115–118.

Kushnirov, V.V. (2000). Rapid and reliable protein extraction from yeast. Yeast *16*, 857–860.

Kutay, U., Ahnert-Hilger, G., Hartmann, E., Wiedenmann, B., and Rapoport, T.A. (1995). Transport route for synaptobrevin via a novel pathway of insertion into the endoplasmic reticulum membrane. EMBO J. *14*, 217–223.

Lang, S., Erdmann, F., Jung, M., Wagner, R., Cavalie, A., and Zimmermann, R. (2011). Sec61 complexes form ubiquitous ER Ca2+ leak channels. Channels (Austin) *5*, 228–235.

Lupas, A., Van Dyke, M., and Stock, J. (1991). Predicting coiled coils from protein sequences. Science *252*, 1162–1164.

Ma, H., Dang, Y., Wu, Y., Jia, G., Anaya, E., Zhang, J., Abraham, S., Choi, J.G., Shi, G., Qi, L., et al. (2015). A CRISPR-based screen identifies genes essential for West-Nile-virus-induced cell death. Cell Rep. *12*, 673–683.

Mariappan, M., Mateja, A., Dobosz, M., Bove, E., Hegde, R.S., and Keenan, R.J. (2011). The mechanism of membrane-associated steps in tail-anchored protein insertion. Nature *477*, 61–66.

Nyathi, Y., Wilkinson, B.M., and Pool, M.R. (2013). Co-translational targeting and translocation of proteins to the endoplasmic reticulum. Biochim. Biophys. Acta *1833*, 2392–2402.

Olsen, J.V., Vermeulen, M., Santamaria, A., Kumar, C., Miller, M.L., Jensen, L.J., Gnad, F., Cox, J., Jensen, T.S., Nigg, E.A., et al. (2010). Quantitative phosphoproteomics reveals widespread full phosphorylation site occupancy during mitosis. Sci. Signal. *3*, ra3.

Pross, E., Soussoula, L., Seitl, I., Lupo, D., and Kuhn, A. (2016). Membrane targeting and insertion of the C-tail protein SciP. J. Mol. Biol. *428*, 4218–4227.

Richard, M., Boulin, T., Robert, V.J., Richmond, J.E., and Bessereau, J.L. (2013). Biosynthesis of ionotropic acetylcholine receptors requires the evolutionarily conserved ER membrane complex. Proc. Natl. Acad. Sci. USA *110*, E1055–E1063.

Sachelaru, I., Winter, L., Knyazev, D.G., Zimmermann, M., Vogt, A., Kuttner, R., Ollinger, N., Siligan, C., Pohl, P., and Koch, H.G. (2017). YidC and SecYEG form a heterotetrameric protein translocation channel. Sci. Rep. *7*, 101.

Satoh, T., Ohba, A., Liu, Z., Inagaki, T., and Satoh, A.K. (2015). dPob/EMC is essential for biosynthesis of rhodopsin and other multi-pass membrane proteins in Drosophila photoreceptors. eLife *4*, e06306.

Schuldiner, M., Metz, J., Schmid, V., Denic, V., Rakwalska, M., Schmitt, H.D., Schwappach, B., and Weissman, J.S. (2008). The GET complex mediates insertion of tail-anchored proteins into the ER membrane. Cell *134*, 634–645.

Seitl, I., Wickles, S., Beckmann, R., Kuhn, A., and Kiefer, D. (2014). The C-terminal regions of YidC from Rhodopirellula baltica and Oceanicaulis alexandrii bind to ribosomes and partially substitute for SRP receptor function in Escherichia coli. Mol. Microbiol. *91*, 408–421.

Sharma, S., Burdon, K.P., Chidlow, G., Klebe, S., Crawford, A., Dimasi, D.P., Dave, A., Martin, S., Javadiyan, S., Wood, J.P., et al. (2012). Association of genetic variants in the TMCO1 gene with clinical parameters related to glaucoma and characterization of the protein in the eye. Invest. Ophthalmol. Vis. Sci. *53*, 4917–4925.

Simon, S.M., and Blobel, G. (1991). A protein-conducting channel in the endoplasmic reticulum. Cell *65*, 371–380.

Simon, S.M., Blobel, G., and Zimmerberg, J. (1989). Large aqueous channels in membrane vesicles derived from the rough endoplasmic reticulum of canine pancreas or the plasma membrane of Escherichia coli. Proc. Natl. Acad. Sci. USA *86*, 6176–6180.

Söding, J., Biegert, A., and Lupas, A.N. (2005). The HHpred interactive server for protein homology detection and structure prediction. Nucleic Acids Res. *33*, W244–W248.

Sojka, S., Amin, N.M., Gibbs, D., Christine, K.S., Charpentier, M.S., and Conlon, F.L. (2014). Congenital heart disease protein 5 associates with CASZ1 to maintain myocardial tissue integrity. Development *141*, 3040–3049.

Spang, A., Saw, J.H., Jørgensen, S.L., Zaremba-Niedzwiedzka, K., Martijn, J., Lind, A.E., van Eijk, R., Schleper, C., Guy, L., and Ettema, T.J.G. (2015). Complex archaea that bridge the gap between prokaryotes and eukaryotes. Nature *521*, 173–179.

Stefanovic, S., and Hegde, R.S. (2007). Identification of a targeting factor for posttranslational membrane protein insertion into the ER. Cell *128*, 1147–1159.

Stefer, S., Reitz, S., Wang, F., Wild, K., Pang, Y.Y., Schwarz, D., Bomke, J., Hein, C., Löhr, F., Bernhard, F., et al. (2011). Structural basis for tail-anchored membrane protein biogenesis by the Get3-receptor complex. Science *333*, 758–762.

Tsirigos, K.D., Peters, C., Shu, N., Käll, L., and Elofsson, A. (2015). The TOPCONS web server for consensus prediction of membrane protein topology and signal peptides. Nucleic Acids Res. *43* (*W1*), W401–W407.

Vilardi, F., Lorenz, H., and Dobberstein, B. (2011). WRB is the receptor for TRC40/Asna1-mediated insertion of tail-anchored proteins into the ER membrane. J. Cell Sci. *124*, 1301–1307.

Vogl, C., Panou, I., Yamanbaeva, G., Wichmann, C., Mangosing, S.J., Vilardi, F., Indzhykulian, A.A., Pangršič, T., Santarelli, R., Rodriguez-Ballesteros, M., et al. (2016). Tryptophan-rich basic protein (WRB) mediates insertion of the tail-anchored protein otoferlin and is required for hair cell exocytosis and hearing. EMBO J. *35*, 2536–2552.

Wang, P., and Dalbey, R.E. (2011). Inserting membrane proteins: the YidC/Oxa1/Alb3 machinery in bacteria, mitochondria, and chloroplasts. Biochim. Biophys. Acta *1808*, 866–875.

Wang, F., Whynot, A., Tung, M., and Denic, V. (2011). The mechanism of tail-anchored protein insertion into the ER membrane. Mol. Cell *43*, 738–750.

Wang, F., Chan, C., Weir, N.R., and Denic, V. (2014). The Get1/2 transmembrane complex is an endoplasmic-reticulum membrane protein insertase. Nature *512*, 441–444.

Wang, Q.C., Zheng, Q., Tan, H., Zhang, B., Li, X., Yang, Y., Yu, J., Liu, Y., Chai, H., Wang, X., et al. (2016). TMCO1 is an ER Ca(2+) load-activated Ca(2+) channel. Cell *165*, 1454–1466.

Wang, S., Sun, S., Li, Z., Zhang, R., and Xu, J. (2017). Accurate de novo prediction of protein contact map by ultra-deep learning model. PLoS Comput. Biol. *13*, e1005324.

Wirth, A., Jung, M., Bies, C., Frien, M., Tyedmers, J., Zimmermann, R., and Wagner, R. (2003). The Sec61p complex is a dynamic precursor activated channel. Mol. Cell *12*, 261–268.

Xin, B., Puffenberger, E.G., Turben, S., Tan, H., Zhou, A., and Wang, H. (2010). Homozygous frameshift mutation in TMCO1 causes a syndrome with craniofacial dysmorphism, skeletal anomalies, and mental retardation. Proc. Natl. Acad. Sci. USA *107*, 258–263.

Yamamoto, Y., and Sakisaka, T. (2012). Molecular machinery for insertion of tail-anchored membrane proteins into the endoplasmic reticulum membrane in mammalian cells. Mol. Cell *48*, 387–397.

Zaremba-Niedzwiedzka, K., Caceres, E.F., Saw, J.H., Bäckström, D., Juzokaite, L., Vancaester, E., Seitz, K.W., Anantharaman, K., Starnawski, P., Kjeldsen, K.U., et al. (2017). Asgard archaea illuminate the origin of eukaryotic cellular complexity. Nature *541*, 353–358.

Cell Reports, Volume *21*

Supplemental Information

Identification of Oxa1 Homologs Operating in the Eukaryotic Endoplasmic Reticulum

S. Andrei Anghel, Philip T. McGilvray, Ramanujan S. Hegde, and Robert J. Keenan

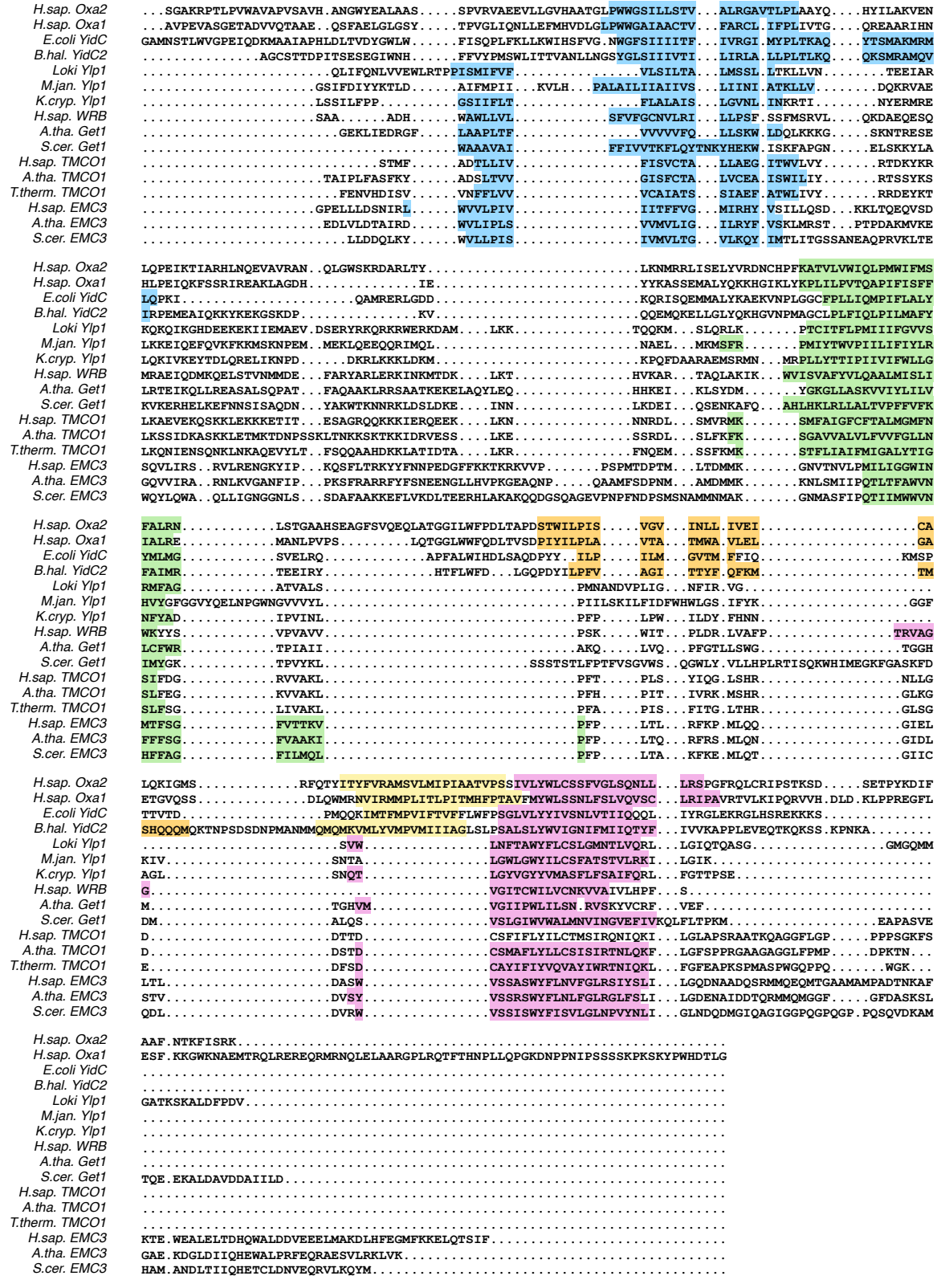

Figure S1. Multiple sequence alignment of members of the Oxa1 superfamily, related to Figure 2. PROMALS3D was used with standard parameters and without any user-defined constraints. TMD predictions from TOPCONS are highlighted; TMDs in the conserved core are colored as in Figure 2, and the additional two TMDs of the Oxa1/Alb3/YidC family are colored orange (TM3) and yellow (TM4).

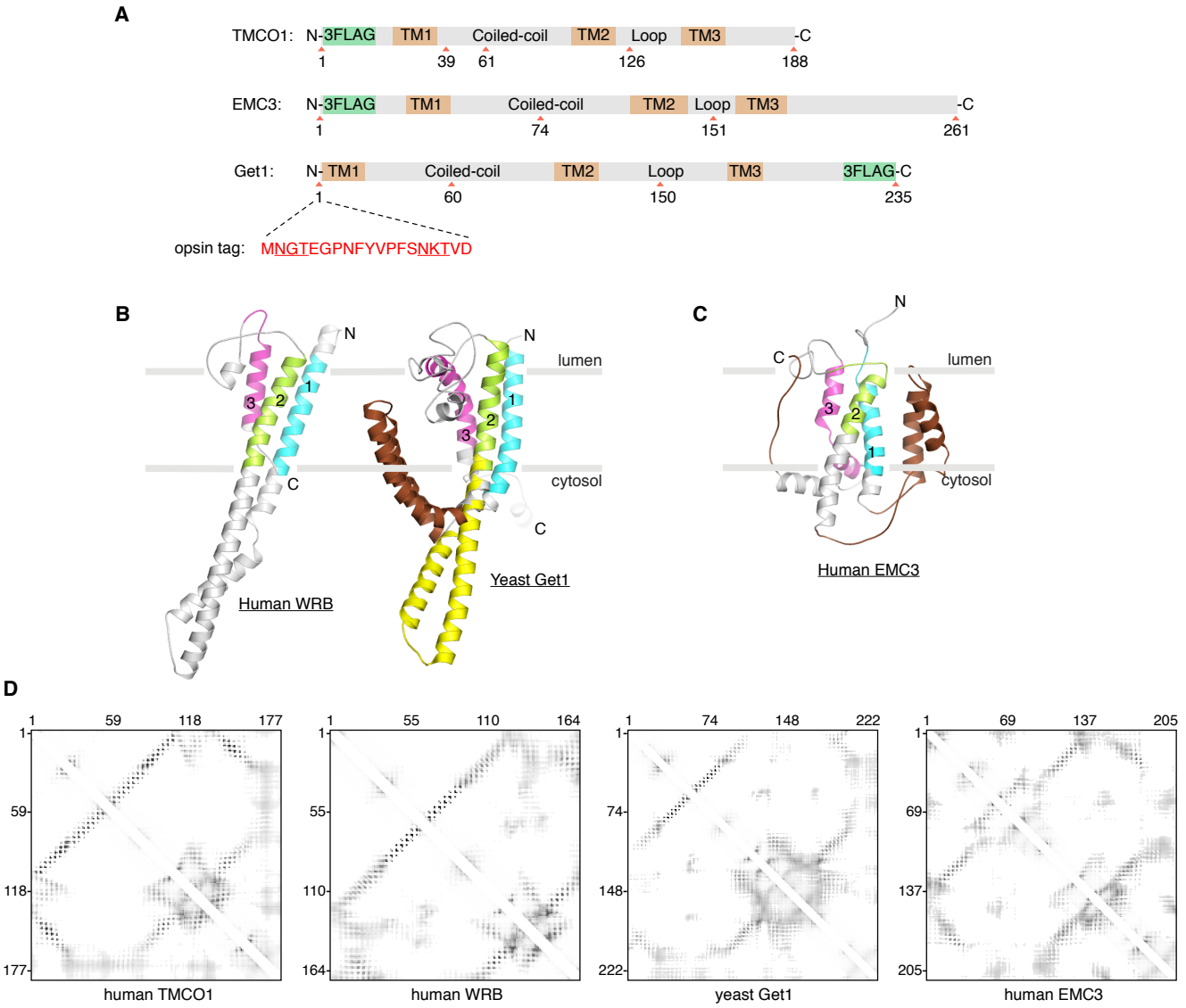

Figure S2. Additional details for the topology mapping experiments and 3D modeling, related to Figure 2. (**A**) Constructs used for glycosylation mapping. An opsin tag (red) containing two N-glycosylation sites (underlined) was inserted at the indicated positions of human TMCO1, human EMC3 and yeast Get1. Tag positions correspond to the native (untagged) sequence. For the TMCO1 and EMC3 constructs, a GSS linker connects the 3xFlag tag and the protein sequence. For the N-terminally opsin-tagged Get1 sequence, a 3xGSS linker was inserted before the first TMD, as sufficient distance from the membrane is required for effective glycosylation. (**B**) Co-variation-based 3D models of human WRB (left) and yeast Get1 (right), as in Figure 2D; note how the highly charged coiled-coil region of yeast Get1 (brown) bends back into the membrane bilayer (grey bars) in a non-physiologic conformation; this is likely due to the lack of a membrane bilayer energy term during 3D modeling (see Methods). In this case, a better, hybrid model is obtained by replacing the distorted coiled-coil (brown) with a crystallographically-defined Get1 coiled-coil (yellow; PDB 3ZS8) by manually docking it as a rigid body between TM1 and TM2 (see also Figure 2D). (**C**) Co-variation based 3D model of human EMC3 colored as in Figure 2D; a coiled-coil motif between TM1 and TM2, and the three TM core are both visible. However, similar to the yeast Get1 model, the coiled-coil and extended C-terminal region (both features colored brown) adopt physically implausible orientations in which they become embedded in the bilayer, despite being highly charged. (**D**) Heat maps of the RaptorX probabilities of two residues being in close proximity (<8 Å); higher probabilities are darker.

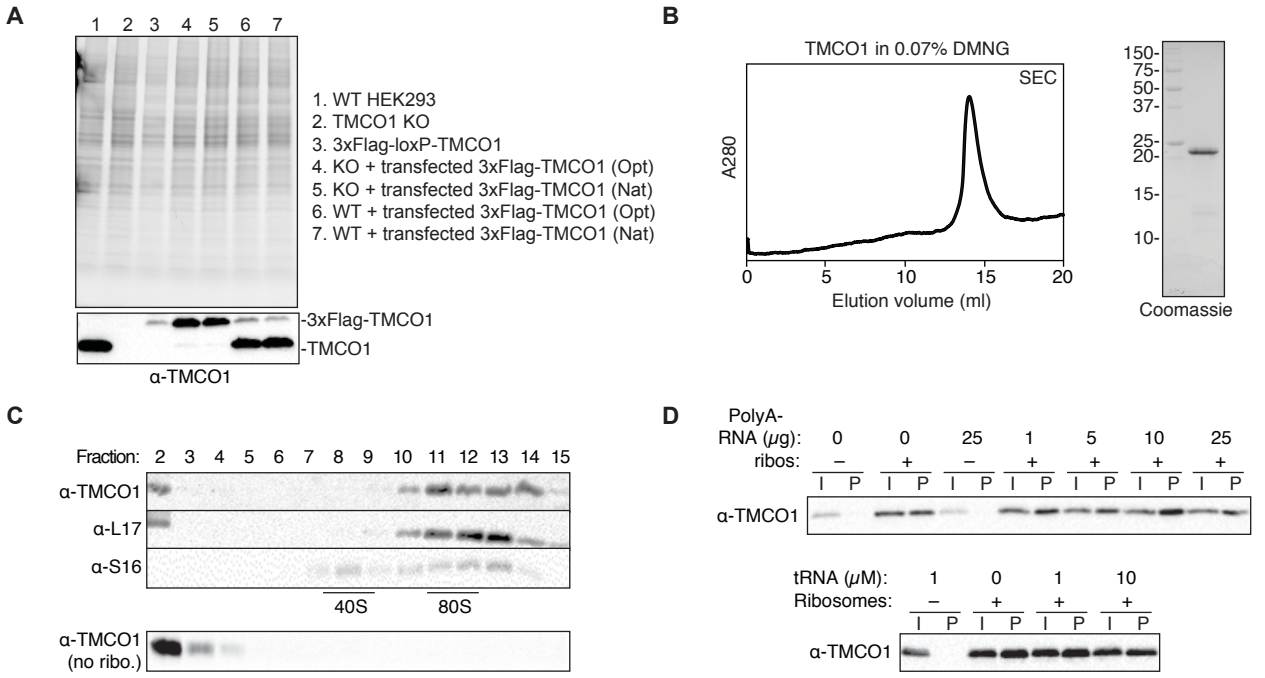

Figure S3. Additional characterization of the ribosome binding properties of TMCO1 in cells and in vitro, related to Figure 3. (**A**) Western blot analysis of TMCO1 expression levels in wild-type (WT) HEK293 cells, CRISPR/Cas9 generated knockout (KO) HEK293 cells, an integrated 3xFlag-tagged TMCO1 cell line and either KO or WT cells transfected with a 3xFlag-tagged TMCO1 construct either with ('Opt') or without ('Nat') codon optimization. A stain-free image of the gel prior to PVDF transfer shows that equal amounts of protein were loaded in each lane. Note that the transfected constructs express at lower levels than endogenous TMCO1 ('WT', lane 1). (**B**) Size-exclusion chromatography (SEC) of Ni-NTA affinity purified, recombinant TMCO1 in DMNG; pooled fractions are shown at right. (**C**) Sucrose gradient analysis of recombinant TMCO1 after chemical crosslinking to nuclease-treated rabbit reticulocyte lysate ribosomes. TMCO1 co-sediments with 80S ribosomes (but not the 40S ribosomal small subunit), while free TMCO1 remains at the top of the gradient. (**D**) Sedimentation analysis of TMCO1-ribosome complexes in the presence of excess competitor RNA; assays contained 1 μM TMCO1, 0.1 μM ribosomes and the indicated concentrations of competitor RNA.

SUPPLEMENTAL EXPERIMENTAL PROCEDURES

Antibodies

Antiserum against human TMCO1 was generated by Lampire Biologicals. Rabbits were immunized with a KLH conjugated EKKKETITESAGRQQKK peptide, located in the cytosolic coiled-coil of TMCO1. Exsanguination bleed was supplemented with 0.02% sodium azide, flash-frozen in liquid nitrogen and stored at -80°C. For immunoprecipitation experiments, antibody was thawed and used immediately without further purification. For western blotting, initial experiments used unpurified serum; other experiments used peptide affinity purified antibody.

Antibodies against L17 (Abgent), S16 (Santa Cruz) and Derlin-1 (Abcam) were purchased, and antibodies against Sec61α and Sec61β were characterized previously (Gorlich et al., 1992).

Cell culture

HEK293-Cas9 cells containing a 3xFlag-Cas9 construct integrated into the genome were generated from HEK293 Flp-In T-REx cells (Invitrogen). A *TMCO1* knockout line derived from these cells was generated at the Genome Engineering Core Facility at the University of Chicago, using a guide RNA with the sequence 5'-GAAACAATAACAGAGTCAGCTGG-3'. Cas9 expression was induced by addition of doxycycline at 10 ng/mL, followed by transfection of a gRNA-expressing plasmid. Single cells were then seeded into 96 well plates allowed to grow clonally. The final *TMCO1* knockout line was verified by both genomic DNA sequencing and immunoblotting with an α-TMCO1 antibody (Figure S3A).

A separate cell line containing an N-terminally Flag tagged TMCO1 was also generated at the same facility using a previously described two step strategy (Xi et al., 2015). The resulting cell line has one nonfunctional TMCO1 allele and one allele containing a 3xFlag-tagged TMCO1 with a 13 amino acid linker (ITSYNVCYTKLSG, from the Cre-lox recombination) before the TMCO1 ORF. The 3xFlag-TMCO1 lines were verified by both genomic DNA sequencing and immunoblotting with α-TMCO1 and α-Flag antibodies (Figure S3A).

Cells were grown in DMEM supplemented with 10% Fetal Bovine Serum (Gemini Benchmark; Lot #A99D00E) and penicillin/streptomycin mixture (Invitrogen). The culture medium was also supplemented with 15 µg/mL Blasticidin and 100 µg/mL Hygromycin B for the *TMCO1* knockout and 3xFlag-TMCO1 cell line generation procedure, but not when growing cells for other applications.

Isolation of total membrane fraction from HEK293 cells

Cells were harvested at a density of 70-100% while growing. Media was removed and cells were scraped into DPBS. Cells were collected by 5 min at 500 x g centrifugation at 4°C, and then lysed osmotically (Sabatini, 2014) by resuspending in a volume of HM Buffer (10 mM Hepes pH 7.5, 10 mM potassium chloride, 1 mM magnesium chloride) equal to 3.5x the volume of the cell pellet. Cells were allowed to swell on ice for 15 minutes, followed by 15 strokes of a douncer

with a tight-fitting pestle (Kontess). Sucrose was then added to 250 mM to balance osmolarity. Nuclei were then removed by pelleting 3 minutes at 700 x g, and the supernatant was centrifuged 10 minutes at 10,000 x g to collect the membrane fraction. Contrary to previous studies, in our hands this was sufficient to pellet most biological membranes of interest, including the endoplasmic reticulum, Golgi, plasma membrane and mitochondria. The membranes were then washed with assay buffer (150 mM potassium acetate, 50 mM Hepes pH 7.4, 5 mM magnesium acetate) and centrifuged again 10 minutes at 10,000 x g to remove any residual cytosolic proteins.

Membranes used for sucrose cushions, gradients, and pull-downs were further treated with micrococcal nuclease to digest polysomes as follows: reaction was supplemented with calcium acetate to 1 mM and 100 Units of micrococcal nuclease (NEB), incubated 10 minutes at 25°C, and then quenched by addition of EGTA to 2 mM. Membranes were then washed again with assay buffer to remove nuclease.

Recombinant TMCO1 production

The gene encoding human TMCO1 was amplified by PCR from total human testicular cDNA (Biosettia), subcloned into a pET28b vector (Novagen) encoding an N-terminal 6xHis tag followed by a TEV protease site, and verified by DNA sequencing. TMCO1 encoding vectors were transformed into E. coli BL21(DE3) and colonies from these transformations were used to inoculated terrific broth (TB, Fisher) starter cultures in baffled flasks containing 50 µg/mL kanamycin. 50 mL starter cultures were grown overnight at 37°C and 250 rpm. 1 L TB cultures containing 50 µg/mL kanamycin were inoculated with 3 mL of starter culture, grown at 37°C, and shaken at 250 rpm until they reached an A_{260} of 0.6. Expression was induced by addition of 0.1 mM isopropyl-β-d-thiogalactoside (IPTG, Sigma) and growth was continued for 4 hrs at room temperature and 250 rpm. Cells were harvested by centrifugation and pellets frozen at -80°C.

Frozen cell pellets were resuspended in 35 mL ice cold lysis buffer (500 mM NaCl, 50 mM Hepes pH 7.5, 10 mM imidazole pH 7.5, 20 µM EDTA pH 8, 1 mM PMSF, 2 mM DTT, 5% glycerol (v/v)) supplemented with 10 µg/mL DNaseI and 0.5 mg/mL of lysozyme. Resuspended pellets were dounced five times on ice and lysed by passages twice through a high pressure microfluidizer. Lysate was clarified by centrifugation at 18,500 x g for 45 min at 4°C. To pellet bacterial membranes, the crude lysate supernatant was subjected to centrifugation at 120,000 x g for 1 hr at 4°C. Pelleted membranes were resuspended gently with a paintbrush in 40 mL ice cold lysis buffer, supplemented with 1% Decyl Maltose Neopentyl Glycol (DMNG, Anatrace), and incubated overnight (~14 hrs) at 4°C with gentle end-over-end mixing. Detergent soluble material was isolated by centrifugation at 120,000 x g for 1 hr at 4°C and batch purified by TALON affinity chromatography (Clonetech). The column was washed with 10 column volumes of lysis buffer supplemented with 15 mM Imidazole pH 7.5 (25 mM Imidazole total) and 0.07% DMNG. Protein was eluted in elution buffer (500 mM NaCl, 50 mM Hepes pH 7.5, 2 mM DTT, 300 mM imidazole pH 7.5, 0.07% DMNG) and further purified by size exclusion

chromatography (Superdex 200, 10/300 GL, GE Healthcare) in 500 mM NaCl, 50 mM Hepes pH 7.4, 2 mM DTT, 0.07% DMNG at room temperature. Desired fractions were pooled and concentrated in a 50 kDa MWCO Amicon ultra centrifugal filter (Millipore). 10% glycerol was added before flash freezing and storage in aliquots at -80°C. Protein concentration was determined by Bradford assay.

Assays for *in vitro* association of TMCO1 with ribosomes

High-salt stripped ribosomes were prepared from rabbit reticulocyte lysate (Green Hectares Farm). After supplementing with 350 mM KCl, the lysate was layered on top of a high density, high salt sucrose cushion (1 M sucrose, 500 mM KCl, 50 mM Tris pH 7.4, 5 mM $MgCl_2$), and subjected to centrifugation at 250,000 x g for 2 hrs at 4°C (TLA100.3, Beckman-Coulter). After incubating the pellet with ribosome buffer (250 mM sucrose, 150 mM KCl, 50 mM Tris pH 7.4, 5 mM $MgCl_2$) for 1 hr on ice, KCl was added to 500 mM and ribosomes were again pelleted through a high density, high salt sucrose cushion. Ribosome pellets were gently resuspended in ribosome buffer, aliquoted, and flash frozen for storage at -80°C.

Ribosome binding assays were carried out in binding buffer (150 mM KCl, 50 mM Tris pH 7.4, 5 mM $MgCl_2$, 0.07% DMNG), with 100 nM purified rabbit reticulocyte ribosomes and a 10-fold molar excess (1 μM) of purified, recombinant TMCO1 in a total volume of 100 μL. After incubating for 1 hr at 4 °C, 80 μL of the binding reaction was pelleted through a sucrose cushion (1 M sucrose, 150 mM KCl, 50 mM Tris pH 7.4, 5 mM $MgCl_2$, 0.07% DMNG) for 2 hr 250,000 x g at 4°C (TLA100.3, Beckman-Coulter). Pellets were washed with 1 mL of ice cold water and resuspended in 40 μL of 1x lithium dodecyl sulphate sample buffer supplemented with 100 mM β-mercaptoethanol. Competition assays were performed as described above, but with the addition of either tRNA or polyA RNA at the indicated concentrations before incubation.

In vitro crosslinking was performed by adding fresh DSP (in DMSO) to a final concentration of 250 μM, followed by incubation for 10 minutes at room temperature. Reactions were quenched by the addition of Tris pH 7.4 to a final concentration of 100 mM, followed by an additional 10 min incubation on ice. NaCl was added to 500 mM to dissociate uncrosslinked TMCO1 from the ribosome. To separate ribosomal subunits after crosslinking, samples were incubated with 2 mM puromycin and 1 mM PMSF for 30 min on ice, then 20 minutes at 37°C. Crosslinked, puromycin-treated samples were separated by centrifugation through a high salt sucrose gradient (10-50% sucrose, 500 mM NaCl, 50 mM Hepes pH 7.5, 0.07% DMNG, 5 mM $MgCl_2$) at 130,000 x g (SW28.1, Beckman-Coulter) for 14 hrs at 4°C. 1 mL fractions were collected manually from the top of the gradient, TCA precipitated, and analyzed by SDS-PAGE.

SUPPLEMENTAL REFERENCES

Gorlich, D., Prehn, S., Hartmann, E., Kalies, K.U., and Rapoport, T.A. (1992). A mammalian homolog of SEC61p and SECYp is associated with ribosomes and nascent polypeptides during translocation. Cell *71*, 489-503.

Sabatini, D.D. (2014). Preparation of crude rough microsomes from tissue culture cells. Cold Spring Harb Protoc *2014*, 980-987.

Xi, L., Schmidt, J.C., Zaug, A.J., Ascarrunz, D.R., and Cech, T.R. (2015). A novel two-step genome editing strategy with CRISPR-Cas9 provides new insights into telomerase action and TERT gene expression. Genome Biol *16*, 231.